Performance of Au-Ag thin film thickness on Surface Plasmon Resonance sensor for heavy metals detection

L. D. MAULUDI[1], R. A. FIRDAUS[1,*], M. YANTIDEWI[1], W. P. TRESNA[2], A. KHUMAENI[3]
[1]Departement of physics, State University of Surabaya (UNESA), Surabaya, Indonesia
[2]National Research and Innovation Agency (BRIN), Tangerang Selatan, Indonesia
[3]Departement of physics, Diponegoro University, Semarang, Indonesia

This study has investigated SPR sensors using plasmonic bimetal, varying the combination of Au-Ag thickness to obtain good sensitivity. In this case, heavy metal analytes are used to test the sensitivity obtained. Simulation and analysis methods were carried out in depth to test the configuration capabilities of each plasmonic bimetal. Although the single Au configuration showed better stability, the Ag characteristics outperformed it in terms of sensitivity. Thus, to obtain optimum sensitivity, the thickness of each plasmonic bimetal was varied with a total thickness remaining at 50 nm. The analysis results show that at thickness variations of 10Au-40Ag nm, the minimum transmittance (T_{spr}) is almost zero. Meanwhile, the thickness variations of 20Au-30Ag nm, 25Au-25Ag nm and 40Au-10Ag nm still have T_{spr} values in the range of 0.2-0.4 nm. Other analysis results show that the thicker the Ag material in the bimetal combination, the narrower the FWHM value of the resulting deep resonance spectrum tends to be. In the variations of heavy metal analytes used such as Cu, Pb, Hg, Zn, Fe and Co, the sensor quality parameters did not show the same trend for each analyte. Overall, the research methodology conducted shows that plasmonic bimetal variations can improve sensor quality parameters for several heavy metal analytes.

(Received August 12, 2024; accepted April 3, 2025)

Keywords: SPR sensors, FDTD, Sensitivity, Au-Ag thickness dependent, Heavy metals

1. Introduction

In recent times, the problem of environmental pollution has been in the spotlight all over the world. In this modern era, urbanization and increasing industrialization are causing a wide spread of various pollutants, including toxic chemicals, pesticides, petroleum products, and heavy metals into natural resources such as water, soil, and air [1]. Heavy metals can be found in water, soil, food, biological samples, and cosmetics. The accumulation of heavy metals in the body has the potential to pose a threat to health and can even cause death if it exceeds normal levels in the body [2], [3]. Today in the environment there are many heavy metals in large quantities such as Cadmium, Lead, Arsenic, Mercury, and Nickel, which create serious problems in the context of the global environment. Heavy metals include toxic essential metals (Cu, Zn, Co, Cr, Mn, and Fe) [4], non-essential metals (Ba, Al, Li, and Zr), less toxic metals (Sn and As), and highly toxic metals (Hg, Cd, and Pb) [5]. Furthermore, several heavy metals were found in marine sediments such as Cr, Pb, and Cu as well as some heavy metals contained in pesticides [6,7]. Heavy metals (Pb, Cr and Cd) are found in foods such as shellfish which, if accumulated in the human body, are not favorable for long-term consumption [8].

Although lead can be found naturally in the environment, the increase in lead content is significantly due to human activities [9]. Lead is released into the air through several sources, including lead mining, factories that use lead compounds, transportation activities, and burning fossil fuels [10]. Lead enters waters or lakes when soil particles are carried away by rainwater. As a result, lead is delivered to animals and plants through air, water, and soil, and this cycle continues an iterative basis [11]. Based on the latest report from the World Health Organization (WHO) in 2021, the Institute for Health Metrics and Evaluation (IHME) projects that half of the 2 million human deaths are caused by Pb exposure globally. Therefore, it is necessary to conduct an analysis related to the presence of heavy metals [12].

Microfabrication technology provides advances in micro-sensors such as the application of optical, chemical, and mechanical systems as molecular sensing devices. One of them is the development of surface plasmon resonance (SPR) sensors. SPR is an optical method that has high sensitivity. This technique operates by stimulating charge waves at the interface between metals, such as Au, Ag, and dielectric materials. Any modification in the optical characteristics of the dielectric layer adjacent to the metal layer affects plasmon activation, which forms the basis of SPR measurements [13]. The sensor is responsive to changes in the refractive index in the environment at the nanometer scale, so it is suitable for detecting heavy metal fiber-optic-based SPRs that may be more miniaturized than using prism-based. Another advantage of fiber-optic based sensors (FO-SPR) is that prism-based SPR sensors are highly sensitive [14]. In optimization, knowledge of plasmonic phenomena FO-SPR sensor design is essential to achieve optimal performance which can also reduce trial and error thereby minimizing costs in experiments. Several numerical methods can be applied to investigate plasmonic phenomena including finite-difference time-domain (FDTD) [15]. Therefore, this study was conducted using the FDTD method with variations in gold and silver thickness dependent.

The factor affecting the sensing performance of the SPR sensor is the metal film. Strong resistance to chemicals and oxidation makes Au an attractive choice for SPR sensors characterized by high stability. However, the inherent high loss of gold sacrifices sensing sensitivity and resolution due to the wide spectrum width [16]. In reverse, Ag allows low loss to improve sensing sensitivity and resolution due to its small imaginary permittivity part [17,18], but it is susceptible to oxidation and easily forms silver sulfide. The Au-Ag bimetal configuration has been used in Kretschmann-type coupler prism sensors with better minimum reflectivity resolution than using a single Au film [17]. Based on the results of research conducted by Du and Zhao, in 2017 showed that the Au-Ag configuration increases the resolution and sensitivity of the sensor due to low Ag loss, while the upper layer of Au to ensure high stability and resistance of the sensor to chemicals and oxidation [19]. The purpose of our research is to observe the effect of gold and silver coating variation on fiber optic based SPR sensor using FDTD simulation method for detection of various heavy metals in Au-Ag thickness variation configuration to get better resolution and sensitivity.

2. Methodology

Here, a 2-dimensional FDTD simulation method is used. The FDTD method can be used to model optical components that have nanoscale structures. In addition to having advantages in ease of understanding however, it requires deep understanding and takes a long time to run a program once and requires a large memory capacity, because it stores a huge amount of grid.

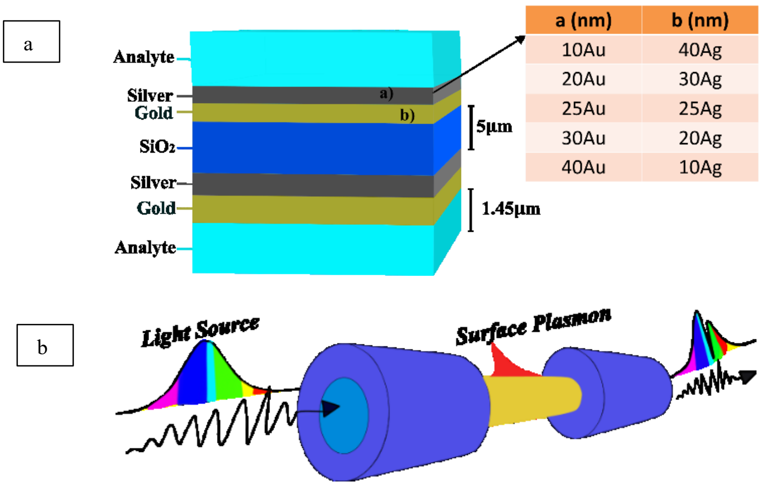

Fig. 1. (a) FO structure of simulation-based heavy metal detection SPR sensor, (b) Fiber Optic-based SPR sensor (colour online)

The FO structure as an SPR sensor is built by designing the geometry and considering the permittivity value of each component involved in the structure. The fiber optic sensor uses single-mode silica optical fiber then coats it with a metal film thereby stimulating the SPR [20]. The permittivity of materials in thin films uses FDTD models integrated in the software, where reference data follow models developed by Johnson and Christy [21]. Then, the wavelength of the light injected into the probe is fixed and set at a wavelength of 200 - 1100 nm. Then, the boundary condition applied with each side is perfectly matched layer (PML). Meanwhile, the mesh type used is auto-nonuniform with a minimum step size of 2 nm. Finally, setting the monitor to record and observe the probe monitor is applied to the simulation type which is 2D X-normal. The simulation time adjusts the size of the simulation area, with auto shutoff also enabled.

Higher sensitivity and better accuracy are always the first choice in designing SPR sensors but due to the poor adsorption ability of metals, a search for materials is still needed to improve sensor performance. SPR active metals Ag, Au, and Cu have been included in research as plasmonic metals in SPR sensors, but Ag oxidation is the main cause of sensor performance degradation [22-26]. Titanium and chromium are often used as adhesive coating materials in SPR sensors. However, there are many drawbacks to these materials, including low optical transmission and metal interdiffusion. These materials produce great sensitivity and a large full-width half maximum (FWHM) value. In addition, these materials show lower transparency because some of the light is absorbed by these materials [27]. Adding another layer of material on top of the metal layer is a solution to overcome oxidation. The addition of an Au layer on top of the Ag layer overcomes the oxidation problem of the Ag layer [19]. Based on Liu et al.'s research, in 2015 to reduce oxidation in the Ag layer, above the Ag layer was given an additional layer of Au that can be deposited epitaxially on top of the Ag layer [28].

3. Result and discussion

In general, metals such as Ag, Al, Au, Cu, In, and others are used as metal films in SPR sensors. Au offers high stability and bioactivity in SPR sensors; however, it results in a wider SPR curve, which negatively impacts the sensor's sensitivity [29, 30]. On the other hand, Ag performs better than Au in SPR sensors because Ag metal films produce narrower resonance peaks, thereby improving the accuracy and sensitivity of SPR sensors [17-33]. Therefore, in this study, we combined Au with an underlying Ag layer to investigate the effect of this combination by varying the thickness of the layers.

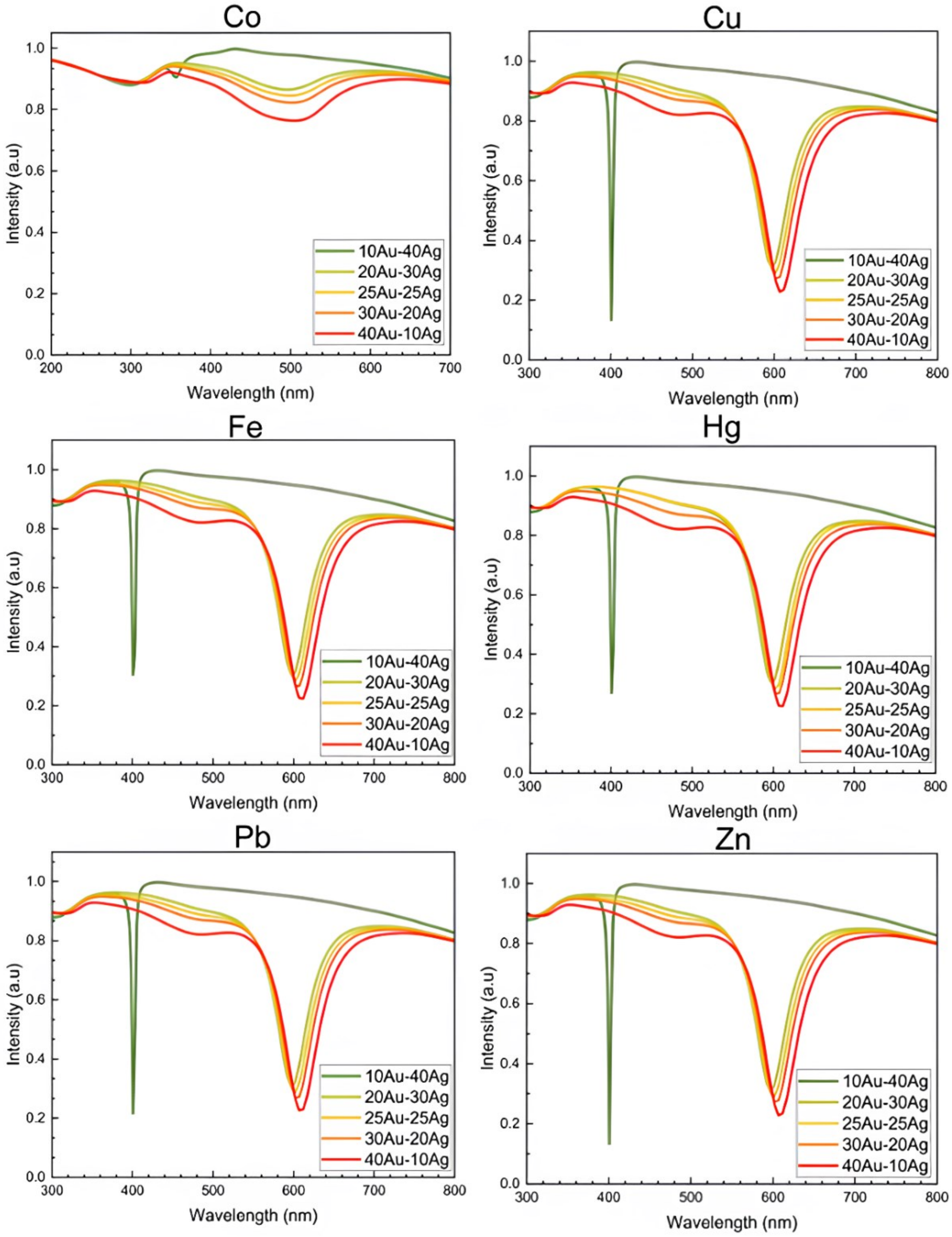

Fig. 2. SPR response transmission spectrum results from the simulation of various heavy metals (Co, Cu, Fe, Hg, Pb, and Zn) with different material layer thickness variations (colour online)

Fig. 2 illustrates the SPR spectrum generated from the FDTD simulation, which was subsequently plotted from the data. It is observed that for heavy metals such as Cu, Fe, Hg, Pb, and Zn, resonance waves appear in the range of 600 – 650 nm. In contrast, cobalt does not exhibit a resonance dip, possibly due to the minimal variation in its concentrations. For variations in material layer thicknesses of 20Au-30Ag nm, 25Au-25Ag nm, 30Au-20Ag nm, and 40Au-10Ag nm, the resulting wavelengths correspond to the range of 600–650 nm, while a thickness of 10Au-40Ag nm produces a wavelength around 400 nm. Furthermore, the several curve parameters were calculated to assess and characterize each curve, including the FWHM (Full Width at Half Maximum). Fig. 3a–3c shows the FWHM values for variations in plasmonic material thickness. It is observed that when the thickness of Au exceeds that of Ag, the FWHM value increases, which reduces the performance of the SPR sensor. A smaller FWHM enhances the performance of such devices.

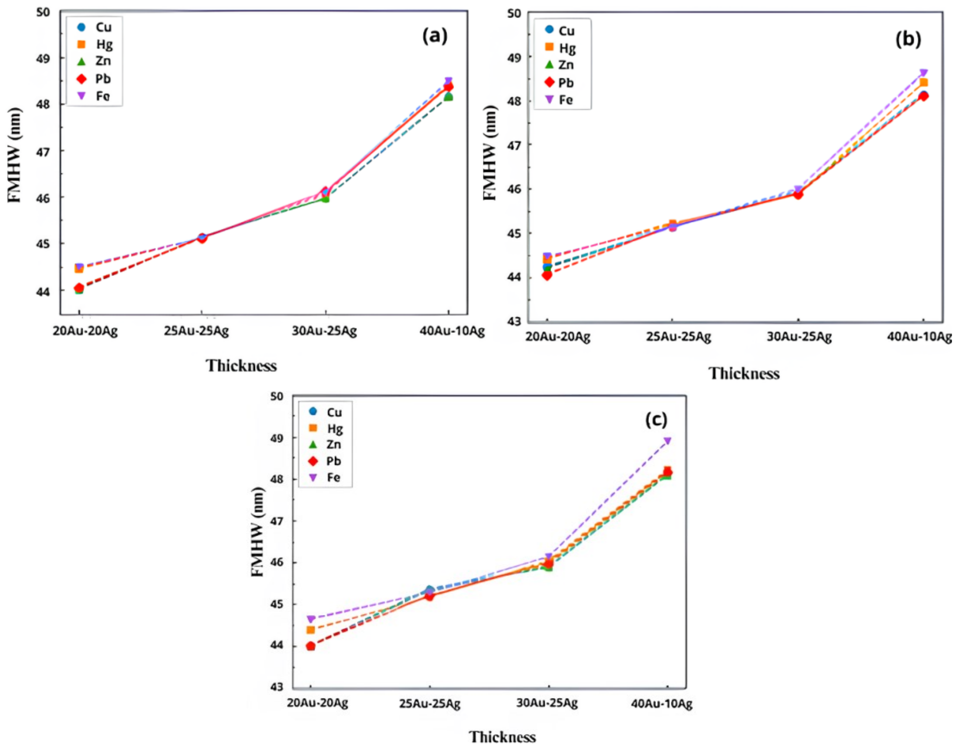

Fig. 3. Characterization of the FWHM curve based on variations in material layer thickness with different heavy metal concentrations: (a) 500 ppm, (b) 700 ppm, (c) 1000 ppm (colour online)

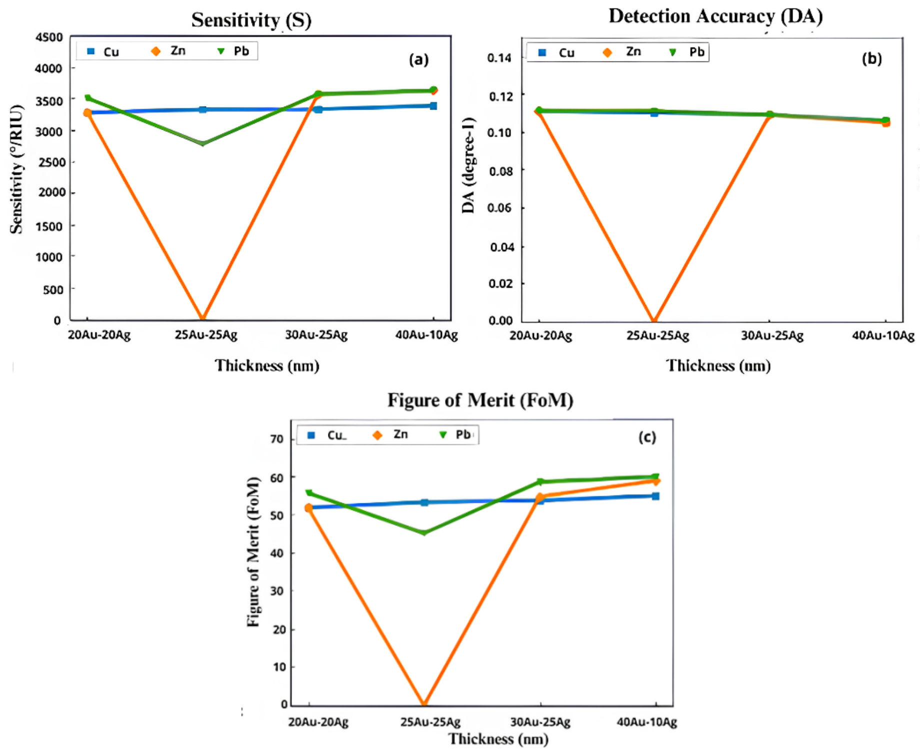

Fig. 4. (a) Sensitivity, (b) Accuracy of Detection and (c) Figure of Merit for heavy metals Cu, Zn and Cu against variation in thickness of plasmonic material (colour online)

In this study, we plotted heavy metals Pb, Cu, and Zn because these three are essential heavy metals frequently found in wastewater. The performance of optical-based SPR sensors depends on several parameters, including sensitivity, selectivity, limit of detection, detection accuracy, resolution, repeatability, reproducibility, noise, range, response time, linearity, drift, quality factor, and figure of merit. However, in simulations, not all parameters can be measured. This section focuses on discussing some measurable parameters in this study, such as sensitivity, detection accuracy, and figure of merit [34], [35].

Performance parameters of the sensor are critical for evaluating its sensitivity in detecting small changes on the surface of the system where biomolecules are adsorbed. The efficiency of an SPR sensor is determined by three main performance parameters: sensitivity (S), figure of merit (FoM), and detection accuracy (DA) [34]. These parameters can be expressed using Equations 1–3:

$$S = \frac{\Delta\lambda spr}{\Delta n} \quad (1)$$

$$DA = \frac{\Delta\lambda spr}{FWHM} \quad (2)$$

$$\text{FoM} = S\left(\frac{1-\text{T}spr}{FWHM}\right) \quad (3)$$

In Equation 1, λspr represents the resonant wavelength, and n is the refractive index value. The refractive index of a medium can influence the direction and speed of light as it crosses the boundary between two different media. Therefore, the refractive index of the analyte is crucial for determining its effect on peak resonance shifts in SPR events. The comparison was made based on an important performance parameter, i.e., the sensitivity of the SPR sensor. Sensitivity is calculated by observing the curve shift with variations in the refractive index (Δn). For the Pb analyte, n values used were 1.3356, 1.3370, and 1.3388.

Fig. 4a shows the relationship between the variation in plasmonic material thickness and sensitivity. The highest sensitivity value, 3.630 nm/RIU, was achieved at a thickness variation of 40Au-10Ag nm for the Zn and Pb analytes. For the Cu analyte, the sensitivity reached 3.390 nm/RIU. Fig. 4b illustrates the variation in detection accuracy (DA) with changes in material thickness. The graph indicates that as the thickness of Au increases, the DA decreases. However, at a thickness variation of 25Au-25Ag nm, no peak shifts were observed, resulting in a sensitivity value as depicted in the graph.

Fig. 4c presents the variation in figure of merit (FoM) values with changes in material thickness. The FoM depends on sensitivity (S), full width at half maximum (FWHM), and minimum transmittance (Tspr) at λspr, as described by Equation 3 A higher S, narrower FWHM, and deeper Tspr result in a higher FoM. Fig. 4 shows that the calculated FoM value at a thickness of 40Au-10Ag nm is approximately 60 nm.

Table 1. Performance parameters for thickness variations with respect to heavy metal variations

Thickness variation (nm)	**Sensitivity (nm/RIU)**		
	Cu	Zn	Pb
20Au-30Ag	3280	3280	3510
25Au-25Ag	3330	0	2780
30Au-20Ag	3330	3570	3570
40Au-10Ag	3390	3630	3630

Thickness variation (nm)	DA		
	Cu	Zn	Pb
20Au-30Ag	0.111	0.111	0.111
25Au-25Ag	0.110	0	0.111
30Au-20Ag	0.109	0.109	0.109
40Au-10Ag	0.105	0.105	0.106

Thickness variation (nm)	**FoM (1/RIU)**		
	Cu	Zn	Pb
20Au-30Ag	51.8	51.8	55.7
25Au-25Ag	53.3	0	45.1
30Au-20Ag	53.7	54.8	58.6
40Au-10Ag	55	58.9	60

Table 2. Performance of FWHM parameters for thickness variations with respect to heavy metal concentration variations at 500 ppm

Thickness variation (nm)	**FWHM**		
	Cu	Zn	Pb
20Au-30Ag	44.0169	44.0169	44.0611
25Au-25Ag	45.1483	45.1483	45.1161
30Au-20Ag	45.9652	45.9652	46.1249
40Au-10Ag	48.1519	48.1519	48.3608

Table 3. Performance of FWHM parameters for thickness variations with respect to heavy metal concentration variations at 700 ppm

Thickness variation (nm)	**FWHM**		
	Cu	Zn	Pb
20Au-30Ag	44.234	44.2115	44.0611
25Au-25Ag	45.1333	45.1267	45.171
30Au-20Ag	45.9151	45.9253	45.8853
40Au-10Ag	48.1519	48.1519	48.1113

Table 4. Performance of FWHM parameters for thickness variations with respect to heavy metal concentration variations at 1000 ppm

Thickness variation (nm)	**FWHM**		
	Cu	Zn	Pb
20Au-30Ag	44.005	44.0169	44.006
25Au-25Ag	45.3449	45.1483	45.2098
30Au-20Ag	45.8865	45.9652	45.9659
40Au-10Ag	48.0922	48.1519	48.1543

Table 1 – Table 4 present the computed values of various important performance parameters of the SPR sensor device with different metal material thicknesses. Table 1 highlights the performance parameters for the SPR sensor when the metal thickness is 40Au-10Ag nm. At this

thickness, the sensitivity reaches 3390 nm/RIU for Cu analytes, while Zn and Pb analytes achieve a sensitivity of 3630 nm/RIU. The limit of detection for the 40Au-10Ag nm thickness variation shows a maximum value and tends to increase, indicating that the detection capability of the system is optimal. Despite achieving the highest sensitivity at this thickness, the detection accuracy (DA) is reduced, which does not meet the criteria for improving the overall performance of the SPR sensor. Tables 2, 3, and 4 detail the performance of the FWHM parameter with varying concentrations of heavy metal analytes across different plasmonic material thicknesses.

4. Conclusion

Measurements on heavy metals have been successfully conducted to determine the effect of adding Ag material on sensor sensitivity. To achieve the highest sensitivity, optimization of the Au-Ag thickness variations was performed. It was observed that at a thickness variation of 10Au-40Ag nm, the minimum transmittance is nearly zero. In contrast, thickness variations of 20Au-30Ag nm, 25Au-25Ag nm, and 40Au-10Ag nm exhibit minimum transmittance in the range of 0.2–0.4. This indicates that when the thickness of the Ag material is greater than that of the Au material, the resulting FWHM tends to be narrower. According to the definition of FWHM, a smaller FWHM value correlates with higher sensor sensitivity. The maximum sensitivity, recorded at a thickness of 40Au-10Ag nm, reached 3.630 nm/RIU. However, for heavy metals such as Co, the resonance wave shift is not significantly noticeable, likely due to the minimal difference in the refractive index (RI) at each concentration. Nevertheless, these findings remain within the framework of plasmonic-coated film environments.

References

[1] Kiran, R. Bharti, R. Sharma, Mater. Today Proc. **51**, 880 (2022).
[2] J. Briffa, E. Sinagra, R. Blundell, Heliyon **6**(9), e04691 (2020).
[3] A. Tjahjono, A. Bambang, S. Anggoro, Journal of Ecological Engineering **18**(2), 7 (2017).
[4] W. Ahmad, R. D. Alharthy, M. Zubair, M. Ahmed, A. Hameed, S. Rafique, Sci. Rep. **11**(1), 17006 (2021).
[5] J. H. Duffus, Pure and Applied Chemistry **74**(5), 793 (2002).
[6] B. Rochaddi, C. A. Suryono, W. Atmodjo, A. Satriadi, IOP Conf. Ser. Earth Environ. Sci. **116**, 012099 (2018).
[7] C. A. Suryono, Jurnal Kelautan Tropis **19**(2), 143 (2016).
[8] N. Heru Suprapti, A. Nur Bambang, F. Swastawati, A. Ni'matullah Al Baari, A. Pramono, J. Teknol. **78**(4–2), 151 (2016).
[9] M. Shahid, Sana Khalid, Ghulam Abbas, Naeem Shahid, Muhammad Nadeem, Muhammad Sabir, Muhammad Aslam, Camille Dumat, "Heavy Metal Stress and Crop Productivity," in Crop Production and Global Environmental Issues, Cham: Springer International Publishing, pp. 1–25, 2015.
[10] A. Violante, V. Cozzolino, L. Perelomov, A. G. Caporale, M. Pigna, J. Soil Sci. Plant Nutr. **10**(3), 268 (2010).
[11] ATSDR, "Toxicological Profile For Lead," 2007.
[12] WHO, "Lead poisoning and health," 2004.
[13] N. A. K. Umiati, K. Triyana, Kamsul, AIP Conf. Proc. **1656**(1), 030012 (2015).
[14] N. Srisittipokakun, J. Kaewkhao, W. Chewpraditkul, P. Limsuwan, Procedia Eng. **32**, 699 (2012).
[15] S. Kumar, Ragini Singh, Zhi Wang, Muyang Li, Xuecheng Liu, Wen Zhang, Bingyuan Zhang, Guoru Li, Results in Optics **10**, 100342 (2023).
[16] S. Y. Wu, H. P. Ho, Proceedings of the IEEE, Electron Devices Meeting, Hong Kong, 2002, pp. 63–68.
[17] B. H. Ong, X. Yuan, S. C. Tjin, J. Zhang, H. M. Ng, Sens. Actuators B Chem. **114**(2), 1028 (2006).
[18] Syifa Avicenna, Iis Nurhasanah, Ali Khumaeni, Indonesia Journal of Chemistry **21**(3), 761 (2021).
[19] W. Du, F. Zhao, Mater. Lett. **186**, 224 (2017).
[20] I. Yulianti, N. M. Dharma Putra, F. Fianti, S. Maimanah, H. Rumiana, M. Y. M. Noor, A. S. M. Supa'at, O. Kurdi, IOP Conf. Ser. Mater. Sci. Eng. **807**(1), 012029 (2020).
[21] P. B. Johnson, R. W. Christy, Phys. Rev. B **6**(12), 4370 (1972).
[22] S. Franzen, The Journal of Physical Chemistry C **112**(15), 6027 (2008).
[23] L. Xia, S. Yin, H. Gao, Q. Deng, C. Du, Plasmonics **6**(2), 245 (2011).
[24] L. C. Oliveira, A. M. N. Lima, C. Thirstrup, H. F. Neff, "Surface Plasmon Resonance Sensors," 2015.
[25] S. Zeng, D. Baillargeat, H.-P. Ho, K.-T. Yong, Chem. Soc. Rev. **43**(10), 3426 (2014).
[26] P. J. Wibawa, M. Nur, M. Asy'ari, W. Wijanarka, H. Susanto, H. Sutanto, H. Nur, Molecules **26**(13), 3790 (2021).
[27] R. Kumar, A. S. Kushwaha, M. Srivastava, H. Mishra, S. K. Srivastava, Appl. Phys. A Mater. Sci. Process. **124**(3), 1 (2018).
[28] H. Liu, T. Liu, L. Zhang, L. Han, C. Gao, Y. Yin, Adv. Funct. Mater. **25**(34), 5435 (2015).
[29] P. R. West, S. Ishii, G. V. Naik, N. K. Emani, V. M. Shalaev, A. Boltasseva, Laser Photon. Rev. **4**(6), 795 (2010).
[30] G. V. Naik, V. M. Shalaev, A. Boltasseva, Advanced Materials **25**(24), 3264 (2013).
[31] J. Hakami, A. Abassi, A. Dhibi, Opt. Quantum Electron. **53**(4), 164 (2021).
[32] S. Singh, A. K. Sharma, P. Lohia, D. K. Dwivedi, Transactions on Electrical and Electronic Materials **23**(3), 254 (2022).
[33] N. Liu, S. Wang, Q. Cheng, B. Pang, J. Lv, Plasmonics **16**(5), 1567 (2021).
[34] V. Yesudasu, H. S. Pradhan, R. J. Pandya, Heliyon **7**(3), e06321 (2021).
[35] B. D. Gupta, S. K. Srivastava, R. Verma, Fiber Optic Sensors Based on Plasmonics, World Scientific, 2015.

*Corresponding author: rohimfirdaus@unesa.ac.id